

Soft Chemical Conversion of Layered Double Hydroxides to Superparamagnetic Spinel Platelets

Yoji Kobayashi,[†] Xianglin Ke,[‡] Hideo Hata,[†] Peter Schiffer,[‡] and Thomas E. Mallouk^{*†}

104 Chemistry Building, Department of Chemistry, and Davey Laboratory, Department of Physics, The Pennsylvania State University, University Park, Pennsylvania 16802

Received December 4, 2007. Revised Manuscript Received January 18, 2008

We report the synthesis of a wide range of single-crystal spinel platelets with exposed (111) faces, lateral dimensions in the micrometer range, and thicknesses of 20–50 nm, prepared by soft chemical dehydration of well crystallized layered precursors. This method enables the synthesis of the metastable composition NiCoAlO₄, which cannot be prepared by conventional solid state synthesis. Because of their nanoscale thickness, mosaic structure, shape anisotropy, and surface porosity, NiCoAlO₄ and NiCo₂O₄ platelets exhibit room-temperature superparamagnetism ($T_B = 40$ and 250 K, respectively) despite the fact that they have micrometer-size lateral dimensions. The accessibility of a wide range of superparamagnetic spinel platelets (as opposed to cubes or spheres) should be useful for studies in ferrofluids and related composite magnetic materials.

Introduction

The layered double hydroxides (LDHs) and brucite-type divalent metal hydroxide salts are a versatile class of lamellar compounds, which can be made to incorporate a broad range of trivalent and/or divalent metal cations. There are numerous reports of thermally decomposing these LDHs into porous mixtures of spinels and other metal oxide phases^{1–4} and a few reports of the phase pure preparation of spinels^{5–9} via a topochemical reaction.¹⁰ However, as a synthetic route to new spinels or to particles of known composition with nanoscale dimensions, this layered precursor method has not yet been exploited. An advantage of this solid-state precursor method is the low temperature of the topochemical transformation, allowing metastable spinels to be prepared. While there is one report commenting that the layered precursor route seems to be useful for metastable compositions,⁹ most of the previous literature describes the synthesis of spinels that are accessible by high-temperature methods. Furthermore, in earlier reports the layered precursors were poorly

crystalline or had rather undefined particle shapes. Recent advances in the synthesis of highly crystalline LDH and brucite-type platelets of various transition metal compositions by Liu, Ma, and others^{11–13} now make it possible to synthesize transition metal LDHs and brucite-type structures as extremely well-defined, single crystalline platelets. These are hexagonally shaped platelets that are typically about 20 nm thick and 1 μm wide, prepared by the homogeneous coprecipitation of metal salts.

Building on these new synthetic developments, we now report the transformation of single-crystalline layered metal hydroxide precursors to spinel products, starting with simple cobalt hydroxide salts and proceeding to ternary LDH precursors. We find that the layered precursor method uniquely permits the synthesis of metastable ternary spinels such as NiCoAlO₄ with well-defined morphology and high crystallinity. Shape studies with anisotropic magnetic particles have been carried out, but they are usually limited to sphere or cube morphologies.¹⁴ The formation of thin spinel platelets with a defined (111) face exposed makes them new targets for basic studies in magnetic anisotropy. The thin crystallite size (20 nm), and perhaps in some cases the porosity of the newly prepared spinel platelets, gives them enhanced properties such as superparamagnetism, which are not typically observed in magnetic particles in the micrometer size range. Because of their superparamagnetism and shape anisotropy, these spinel platelets may exhibit interesting characteristics as ferrofluids, magnetic liquid crystalline colloids, or in magnetorheology. Thin films of spinel are also

* Corresponding author. E-mail: tom@chem.psu.edu.

[†] Department of Chemistry, The Pennsylvania State University.

[‡] Department of Physics, The Pennsylvania State University.

- (1) Sun, G.; Sun, L.; Wen, H.; Jia, Z.; Huang, K.; Hu, C. *J. Phys. Chem. B* **2006**, *110*, 13375–13380.
- (2) Zou, L.; Li, F.; Xiang, X.; Evans, D. G.; Duan, X. *Chem. Mater.* **2006**, *18*, 5852–5859.
- (3) Ruano-Casero, R. J.; Perez-Bernal, M. E.; Rives, V. *Z. Anorg. Allg. Chem.* **2005**, *631*, 2142–2150.
- (4) Kannan, S.; Venkov, T.; Hadjiivanov, K.; Knözinger, H. *Langmuir* **2004**, *20*, 730–736.
- (5) Meng, W.; Li, F.; Evans, D. G.; Duan, X. *Mater. Chem. Phys.* **2004**, *86*, 1–4.
- (6) Markov, L.; Petrov, K. *React. Solids* **1986**, *1*, 319–327.
- (7) Liu, J.; Li, F.; Evans, D. G.; Duan, X. *Chem. Commun.* **2003**, 542–543.
- (8) Li, F.; Liu, J.; Evans, D. G.; Duan, X. *Chem. Mater.* **2004**, *16*, 1597–1602.
- (9) Rojas, R. M.; Kovacheva, D.; Petrov, K. *Chem. Mater.* **1999**, *11*, 3263–3267.
- (10) Markov, L.; Petrov, K.; Lyubchova, A. *Solid State Ionics* **1990**, *39*, 187–193.

- (11) Liu, Z.; Renzhi, M.; Osada, M.; Takada, K.; Sasaki, T. *J. Am. Chem. Soc.* **2005**, *127*, 13869–13874.
- (12) Ma, R.; Liu, Z.; Takada, K.; Iyi, N.; Bando, Y.; Sasaki, T. *J. Am. Chem. Soc.* **2007**, *129*, 5257–5263.
- (13) Liu, Z.; Ma, R.; Ebina, Y.; Iyi, N.; Takada, K.; Sasaki, T. *Langmuir* **2007**, *23*, 861–867.
- (14) Song, Q.; Zhang, Z. *J. Am. Chem. Soc.* **2004**, *126*, 6164–6168.

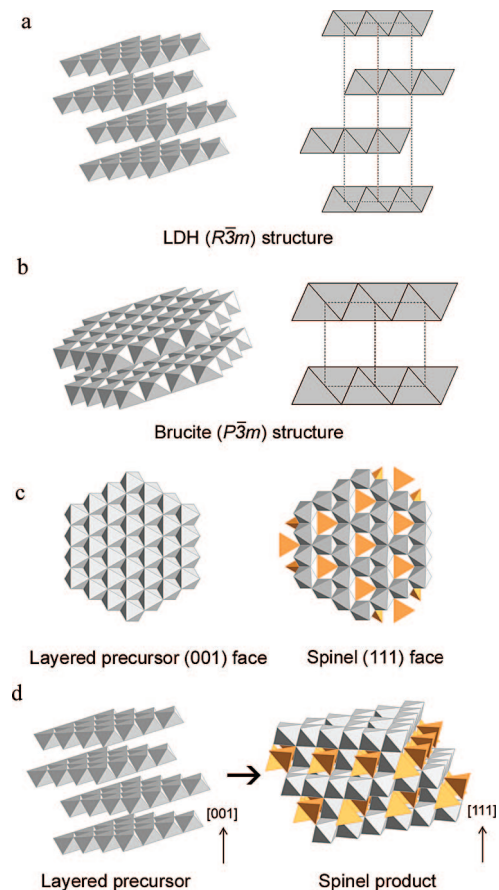


Figure 1. Diagrams of the (a) LDH structure, (b) brucite structure, (c) LDH (001) and spinel (111) faces, and (d) transformation from LDH platelet to spinel platelet with the (111) face exposed. Interlayer species have been omitted from the polyhedral representations of the structures.

interesting for spintronics applications,¹⁵ and these thin platelets may serve as building blocks for growing thin films under mild wet chemical conditions.

The LDH (hydroxylated) structure consists of edge-sharing octahedral layers as shown in Figure 1a. This type of structure is rhombohedral ($R\bar{3}m$) and consists of three layers within the unit cell along the c -axis, and so is sometimes referred to as the $3R_1$ polytype. Most LDHs crystallize in this structure, although some LDHs can crystallize as $3R_2$, $2H_1$ (as in the mineral manasseite), or $1H$ polytypes.¹⁶ β -Ni(OH)₂ and Fe(OH)₂ are also known to crystallize in the same $3R_1$ type structure, and the structure of α -Co(OH)₂ is similar.¹⁷ β -Co(OH)₂, however, crystallizes in a brucite structure ($P\bar{3}m$), in which the layer stacking is different (1H) as shown in Figure 1b.

The symmetry of the individual sheets closely resembles that of the (111) planes of the $Fd\bar{3}m$ spinel structure, shown in Figure 1c. We postulate that as the LDH is dehydrated and some of the metal ions are oxidized, ions within the octahedral layers leave to fill some of the interlayer sites and become the tetrahedrally coordinated cations of the spinel

structure. The closely related symmetry of the LDH layers and spinel (111) planes permits the reaction to be fairly topotactic (within the precursor layer dimensions, at least), and as Markov et al. observed, one expects the 3-fold axis of the LDH precursor to coincide with the [111] axis of the spinel product, as shown in Figure 1c.¹⁰

Results and Discussion

Our initial hypothesis was that the layered metal hydroxide method might yield spinels with both metastable cation distributions and compositions. In order to test this idea, a range of the binary and ternary LDHs Co₂Al-LDH, FeCoAl-LDH, ZnCoAl-LDH, NiCoAl-LDH, Ni₂Al-LDH, and structurally similar Ni_{1/3}Co_{2/3}(OH)₂, α -Co(OH)₂, and β -Co(OH)₂ were synthesized as highly crystalline platelets. In general, IR analysis indicated that both nitrate and carbonate anions together with water were intercalated, although no attempts were made to quantify the relative amounts. Elemental analyses were also conducted on select samples to determine relative metal cation ratios, with ratios reasonably close to the nominal amount for NiCoAl-LDH and Ni_{1/3}Co_{2/3}(OH)₂ (see the Supporting Information for IR and ICP-AES results). Dehydrating these LDHs in an oxidizing environment (i.e., in oxygen) led to spinels for all cases except Ni₂Al-LDH. However, we did not find any unusual cation distributions for cases such as Co₂AlO₄ and ZnCoAlO₄. Determining cation distributions in other spinel products containing Ni, Co, and Fe were difficult due to similar atomic scattering factors. For the LDH precursors, there is some EXAFS, IR, and UV-vis evidence that supports long-range ordering in certain compositions (Cr-containing LDHs,^{18–20} aged Mg-Al LDHs,²¹ and other systems¹⁶), which may have an interesting effect on the cation distribution of the spinel product. However, ordering of this type is difficult to detect by XRD because the superstructure lines can be very weak (for example, the superstructure line for the Zn₂Cr-Cl LDH is calculated to be only 0.1% of the strongest reflection), and we did not observe any superstructure reflections in our own XRD patterns.

We did find that the ternary LDH Ni_{1/3}Co_{1/3}Al_{1/3}(OH)₂·(CO₃²⁻)_x·(NO₃⁻)_y·nH₂O decomposes to a metastable spinel (NiCoAlO₄) that decomposes above 600 °C. Furthermore, we find that this spinel cannot be prepared by alternate methods of coprecipitation or solid state reaction; it is only accessible from a well-crystallized LDH precursor.

Figure 2 shows the TEM images of the LDH platelets and their SAED patterns, showing the transition from the rhombohedral/hexagonal LDH to a face-centered cubic spinel platelet. Although there appear to be two overlapping LDH platelets in Figure 2a, the corresponding SAED pattern shows that they are probably two fused crystallites oriented epitaxially. The pattern shown is characteristic of the [001] zone

(15) Lüders, U.; Barthélémy, A.; Bibes, M.; Bouzouane, K.; Fusil, S.; Jacquet, E.; Contour, J.-P.; Bobo, J.-F.; Fontcuberta, J.; Fert, A. *Adv. Mater.* **2006**, *18*, 1733–1736.
 (16) Bellotto, M.; Rebours, B.; Clause, O.; Lynch, J.; Bazin, D.; Elkaim, E. *J. Phys. Chem.* **1996**, *100*, 8527–8534.
 (17) Ma, R.; Liu, Z.; Takada, K.; Fukuda, K.; Ebina, Y.; Bando, Y.; Sasaki, T. *Inorg. Chem.* **2006**, *45*, 3964–3969.

(18) Roussel, H.; Brioso, V.; Elkaim, E.; de Roy, A.; Besse, J. P. *J. Phys. Chem. B* **2000**, *104*, 5915–5923.
 (19) Roussel, H.; Brioso, V.; Elkaim, E.; de Roy, A.; Besse, J. P.; Jolivet, J. P. *Chem. Mater.* **2001**, *13*, 329–337.
 (20) Boclair, J. W.; Braterman, P. S.; Jiang, J.; Lou, S.; Yarberr, F. *Chem. Mater.* **1999**, *11*, 303–307.
 (21) Richardson, M. C.; Braterman, P. S. *J. Phys. Chem. C* **2007**, *111*, 4209–4215.

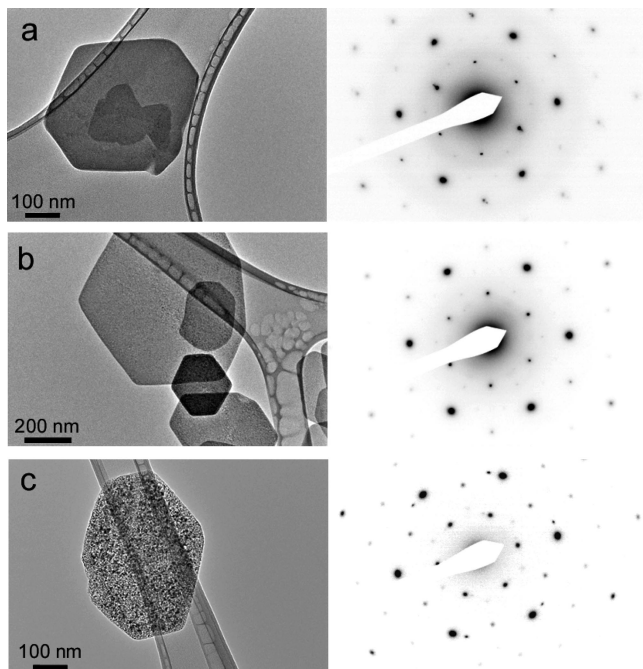


Figure 2. TEM images and diffraction patterns of (a) NiCoAl-LDH, (b) product after treatment at 250 °C, 15 min, (c) at 500 °C, 12 h.

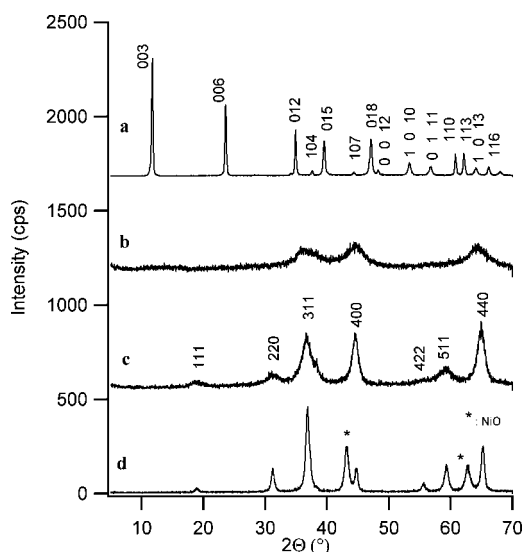


Figure 3. XRD patterns of (a) NiCoAl-LDH, (b) product after treatment at 250 °C, 15 min, (c) at 500 °C, 12 h, and (d) at 800 °C, 12 h.

axis in hexagonal coordinates, and d_{110} obtained from the pattern is approximately 1.50 Å. Heating the platelets to 250 °C under flowing oxygen atmosphere leads to no apparent change (Figure 2b), although maintaining this temperature for 12 h gave a mixture of spinel ([111] zone axis) and LDH [001] spots (not shown). Further heating to 500 °C gave only spinel spots, where $d_{440} = 1.45$ Å, corresponding to a cubic lattice parameter of $a = 8.20$ Å. In general, TEM images of platelets viewed along their edges show that they are approximately 20 nm thick.

The series of X-ray diffraction patterns in Figure 3 show the same transition. The top pattern of the LDH precursor shows that the platelets are highly crystalline. The strong intensities of the 012, 015, 018, and 1 0 10 reflections imply that the individual layers are well ordered to form the 3R₁

polytype.²² Using hexagonal indices, the lattice parameters for this LDH are $a = 3.045$ Å, $c = 22.6$ Å, and the (rhombohedral) space group is $R\bar{3}m$. The hexagonal a parameter implies a d_{110} of 1.52 Å, which is reasonably close to that observed by TEM (1.50 Å). When this compound is heated to 250 °C, the XRD pattern (Figure 3b) shows that the LDH structure is already lost and the spinel structure has started to form; this is slightly different from the description given by the electron diffraction, which indicates that the structure at this stage is still that of the LDH precursor. Further heating to 400 or 500 °C shows spinel formation according to XRD, as the electron diffraction patterns also show. However, heating the sample to 800 °C shows a clear decomposition to produce a new phase with Ni-O type structure and a similar cubic lattice parameter coexisting with a spinel phase. Given the thermodynamic stability of NiO in the rocksalt structure and the tendency of NiCo₂O₄ to decompose at high temperatures, it is not surprising that NiO or (Ni_xCo_{1-x})O might segregate. If this is the case, the remaining spinel phase should be close to a Co₂AlO₄ or CoAl₂O₄ type spinel. TEM images of NiCoAlO₄ after decomposition at 800 °C (see the Supporting Information) show a heterogeneous mixture of numerous platelets, cubes and spherical particles a few hundred nanometers in width. SAED patterns show that the cubes/spheres have a cubic structure, and EDS shows them to contain chiefly Ni and Co. Larger, fairly amorphous aggregations of plates were also observed, and EDS indicated that they contained primarily Al.

High-resolution imaging of the spinel platelets shows lattice fringes running over tens to hundreds of nanometers, as seen in Figure 4. The top picture in Figure 4 is a view looking at the edge of a NiCoAlO₄ platelet, whereas the bottom picture is a view of the face of the platelet. Lattice fringes can be seen running long distances (beyond the field of view in the shown image), despite the porous, rough surface induced during transformation to the spinel. The rough surface induces a high surface area conversion from the LDH precursor to the spinel product increased the BET surface area from 20 to 120 m²/g. Assuming a density of 5.2 g/cm³, a solid spinel platelet 20 nm thick and 1 μm² in area would be expected to have a surface of only 20 m²/g, close to that of the precursor.

Each spinel product exhibits a single set of electron diffraction spots and long lattice fringes, consistent with a single crystal platelet. However, close examination of the diffraction spots implies that the platelets possess a mosaic structure, with small crystallites slightly misaligned with respect to each other. Figure 5 shows magnified view of diffraction spots from the (a) LDH and (b) spinel product, respectively. While the diffraction spot for the LDH precursor is circular, the spots from the spinel product are elongated along a constant d -spacing (i.e., along concentric arcs). Profiling the spots as shown in the lower portion of Figure 5 shows the different peak widths, and this difference was observed for numerous spots in multiple spinel platelets. It

(22) Radha, A. V.; Shivakumara, C.; Vishnu Kamath, P. *Clays Clay Miner.* **2005**, *53*, 520–527.

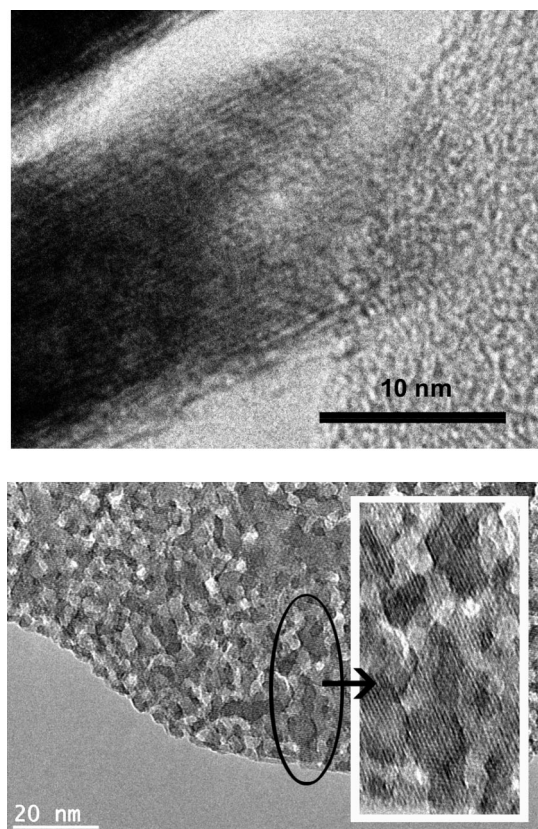


Figure 4. High-resolution TEM images of a NiCoAlO₄ platelet formed at 500 °C.

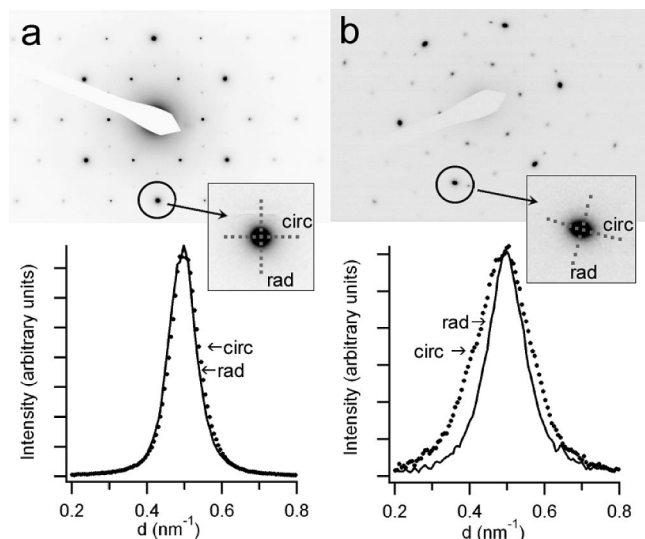


Figure 5. Profiles of diffraction spots from (a) a NiCoAl-LDH platelet and (b) NiCoAlO₄ spinel platelet.

is highly possible that the apparent mosaic structure is related to the porous, rough surface of the platelet.

The acute observer will also find that the electron diffraction patterns of the (111) zone of NiCoAlO₄ prepared at 500 °C show sharp spots, whereas all the peaks in the corresponding X-ray diffraction pattern are quite broad. For example, the platelets are about 500 nm to 1 μm wide and the SAED pattern (always recorded with the selective area aperture covering at least 50% of a platelet) shows only a single set of sharp spots, as in the {440} spots (the six darkest spots in Figure 5b). However, in the X-ray pattern (as in

Figure 3c) the 440 reflection at 65° implies a crystallite size of only 9 nm. The mosaic structure suggested by the elongated diffraction spots is one factor that contributes to peak broadening in the X-ray diffraction pattern. However, the primary reason for the broad X-ray peaks is that XRD and SAED are probing crystallinity in different directions; that is, SAED probes in-plane crystallinity only, whereas X-ray peak widths include symmetry-equivalent cross-plane reflections. Because of the high symmetry of the cubic spinel system, there are many planes of the {440} family; some of these are perpendicular to the platelet face and therefore reflect the long-range in-plane crystallinity. Many others lie at oblique angles with respect to the platelet face. Only the {440} planes perpendicular to the platelet contribute to electron diffraction, whereas all {440} planes contribute to the X-ray diffraction pattern. In the X-ray pattern the broad peaks from oblique {440} planes are superimposed on a smaller component of sharp {440} peaks, resulting in an overall broad peak shape.

Although the XRD in Figure 3c shows no detectable NiO impurity in the NiCoAlO₄ platelets, the elemental homogeneity of the platelets is still somewhat open to question. An attempt was made to acquire element-specific high resolution TEM images using an energy filter. However, interpretation proved to be difficult because of the weak signal and the heterogeneous contrast caused by surface roughness.

NiCo₂O₄ is a spinel related to NiCoAlO₄ which is also known to decompose to NiO and a Ni-deficient spinel above usually 400–500°. ^{23,24} However, NiCo₂O₄ is quite accessible by conventional methods such as heating nitrate salts to 350 °C or coprecipitating amorphous metal hydroxides and then calcining them at similar temperatures. To test if the ternary NiCoAlO₄ spinel could be made by other methods, we tried three different procedures: (1) direct solid-state synthesis from nitrate salts, (2) the citrate gel method, and (3) from an amorphous hydroxide precipitate of the metal salts. The first two methods produced a mixture of a NiO and spinel type phase, as shown in XRD patterns a and b in Figure 6. The hydroxide precipitate did form a spinel phase without any noticeable NiO-type phases (Figure 6c), but the TEM image Figure 6e shows that the crystallites are extremely small and aggregate to form larger particles. These control experiments show that the layered precursor method is the only way thus far to prepare highly crystalline samples of NiCoAlO₄; it may be the ternary nature of this system that makes it more difficult to prepare phase-pure than NiCo₂O₄.

When examining different spinel products, we found that the α-Co(OH)₂ precursor gave lacey spinel platelets that were still reminiscent of the original hexagonal plate morphology. What is surprising is that despite the excessive deformation, each platelet still remains a single crystal. The Co₃O₄ spinel platelets formed from the β precursor are also single crystalline, but have some cracks, as opposed to the lacey structure. Dehydrating both precursors at a slower rate of 1

- (23) Battle, P. D.; Cheetham, A. K.; Goodenough, J. B. *Mater. Res. Bull.* **1979**, *14*, 1013–1024.
 (24) Marco, J. F.; Gancedo, J. R.; Gracia, M.; Gautier, J. L.; Ríos, E. I.; Palmer, H.; Greaves, C.; Berry, F. J. *J. Mater. Chem.* **2001**, *11*, 3087–3093.

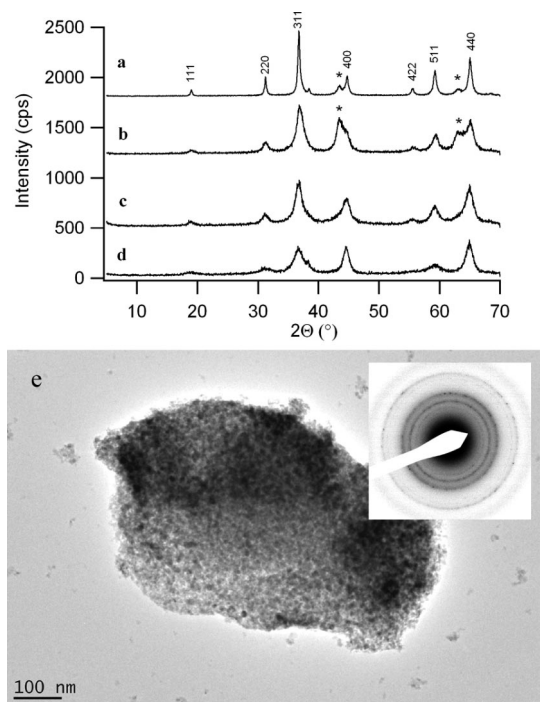


Figure 6. XRD of attempted NiCoAlO_4 synthesis from (a) solid-state reaction of nitrate salts, (b) citrate gel method, (c) amorphous metal hydroxides, (d) crystalline LDH precursor, and (e) TEM image of product from (c).

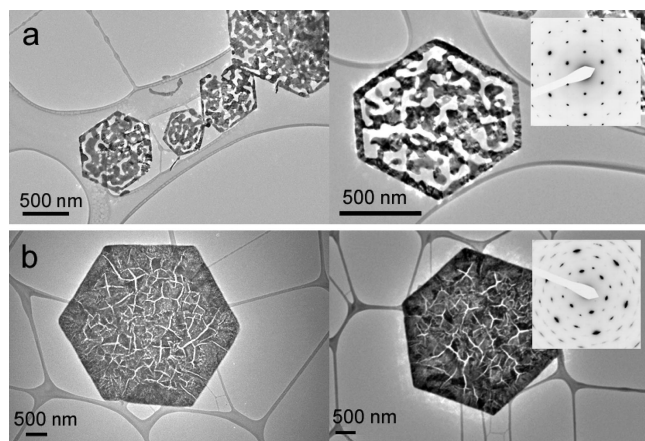


Figure 7. TEM images and diffraction patterns of Co_3O_4 platelets formed from (a) $\alpha\text{-Co(OH)}_2$ and (b) $\beta\text{-Co(OH)}_2$.

$^\circ/\text{min}$ (compared to the $10^\circ/\text{min}$ used in other experiments) did not result in any changes in the final morphology.

It is likely that this lacy platelet is an extreme case of the surface roughness induced in the NiCoAlO_4 case. Despite the transformation to spinel being nominally topochemical, a slight decrease in the in-plane lattice parameter is necessary during transformation to spinel, which is probably the cause of roughness or, in the case of Co_3O_4 , extreme porosity. When one compares the LDH and spinel (111) layers closely; the spinel (111) layers have a higher metal cation density per unit area. Panels c and d in Figure 1 illustrate that the spinel (111) layers are composed of two alternating sublayers; one is the purely octahedral (gray) layer and the other is the layer composed of both gray octahedra and peach-colored tetrahedra. As mentioned earlier and shown in Figure 1c, one can imagine how metal ions in select octahedra in the

precursor move to form the octahedral/tetrahedral sublayer. However, when one counts the cation holes in the octahedral layer and compares it to the cations per area of the octahedral/tetrahedral layer, there are two extra cations per unit area in the latter. To form a large crystallite of the ideal spinel structure would require long-range diffusion of metal atoms to provide these extra cations, accompanied by shrinkage of the crystallite in the in-plane direction. An alternate view of the transformation is that two neighboring LDH sheets (as opposed to a single sheet) form a pair of the octahedral and octahedral/tetrahedral layers; however, the total number of cations per unit area during the transformation is again not conserved.

Magnetic Properties of Platelets of NiCoAlO_4 and NiCo_2O_4 . Since small particles of ferrimagnetic materials can exhibit superparamagnetism, an interesting question is whether these thin platelets are superparamagnetic or ferrimagnetic. While their thickness is within range of room-temperature superparamagnetism, their lateral dimensions are very large. To date, there have been some studies of shape control of superparamagnetic particles, but most of these focus on cubes or spheres.¹⁴ To examine the effect of the platelet morphology on magnetism, a comparison was made between NiCo_2O_4 in platelet form and bulk powder form. NiCo_2O_4 is a known ferrimagnet (T_c ranging 350K–670K^{23,25–28}) with an extrapolated 0 K saturation magnetization of 1.25–1.5 μ_B per formula unit, depending on the synthetic route.^{23,24,27,29} Previously, Markov et al. and Klissurski et al. have prepared NiCo_2O_4 from layered precursors, but they did not examine the morphology or magnetic properties of their spinel products.^{6,30}

Isotropic (1–2 μm diameter) particles of NiCo_2O_4 were prepared at 350 and 500 $^\circ\text{C}$. Although these bulk NiCo_2O_4 samples partially decompose at 500 $^\circ\text{C}$ to produce a small amount of NiO impurity, magnetic measurements were conducted on samples prepared at both temperatures since the platelets could be made at 500 $^\circ\text{C}$ without any NiO impurity (see the Supporting Information). Both bulk NiCo_2O_4 samples showed similar magnetic behavior, consistent with ferrimagnetism below its Curie temperature and a saturation magnetic moment of 1.5 μ_B (2 K) (see the Supporting Information for magnetization data).

In contrast, NiCo_2O_4 in platelet form (approximately 1 μm lateral dimensions and 50 nm thick) showed superparamagnetism with a blocking temperature T_B of approximately 250 K, as shown in Figure 8a; the zero-field-cooled lines and field-cooled lines match well above T_B . Hysteresis curves above and below T_B show the absence and presence of hysteresis, respectively. The saturation magnetization at 2 K is approximately 1.3 μ_B , close to that of isotropic powdered

(25) Holgersson, S.; Karlsson, A. *Z. Anorg. Allg. Chem.* **1929**, *183*, 383–394.

(26) Blasse, G. *Philips Res. Rep.* **1963**, *18*, 383–392.

(27) Lenglet, M.; Guillaumet, R.; Durr, J.; Gryffroy, D.; Vandenberghe, R. E. *Solid State Commun.* **1990**, *74*, 1035–1039.

(28) Knop, O.; Reid, K. I. G.; Sutarno, Y.; Nakamura, Y. *Can. J. Chem.* **1968**, *46*, 3463–3476.

(29) Marco, J. F.; Gancedo, J. R.; Gracia, M.; Gautier, J. L.; Rios, E.; Berry, F. J. *J. Solid State Chem.* **2000**, *153*, 74–81.

(30) Klissurski, D. G.; Uzunova, E. L. *Chem. Mater.* **1991**, *3*, 1060–1063.

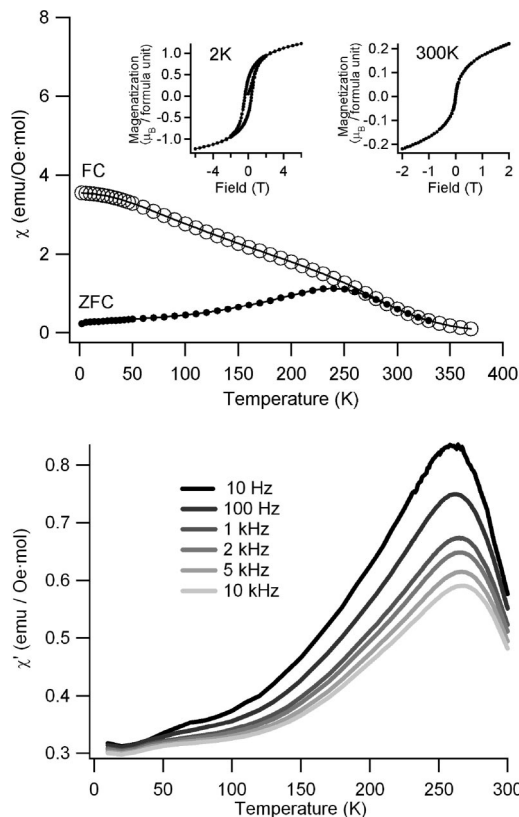


Figure 8. (a) DC magnetization data on NiCo_2O_4 platelets and (b) AC magnetic susceptibility data on the same sample.

NiCo_2O_4 . AC susceptibility measurements in Figure 8b show the increase of T_B as the frequency of the applied field increases, which is another indication of superparamagnetism.

Similar measurements were also done on the metastable NiCoAlO_4 platelets (see Figure 9). They showed similar superparamagnetic behavior, with a lower blocking temperature (30–40 K) probably because the platelets were thinner (20 nm). In the field cooled curve for Figure 8a the increase in susceptibility at low temperatures is somewhat suppressed, and a similar trend can be seen in Figure 9a also. This may be attributed to domain–domain interactions within the platelet, and to a lesser extent between separate platelets; however, we believe that in our case, this interaction does not lead to spin glass formation as other authors have found.^{31,32} The temperature dependence of the heat capacity of the NiCoAlO_4 platelets was measured (see the Supporting Information), and no change in sign of the slope was observed near 40K. The fact that no change was observed excludes the possibility of the 40K event being a spin glass or ferrimagnetic transition. This result, combined with the AC susceptibility data, supports our conclusion that the peak in the zero-field-cooled peak at 40K is indeed at blocking temperature.

The blocking temperatures of these two compositions of spinel platelets are quite different and in general are very low considering the large volume of the platelets. Although

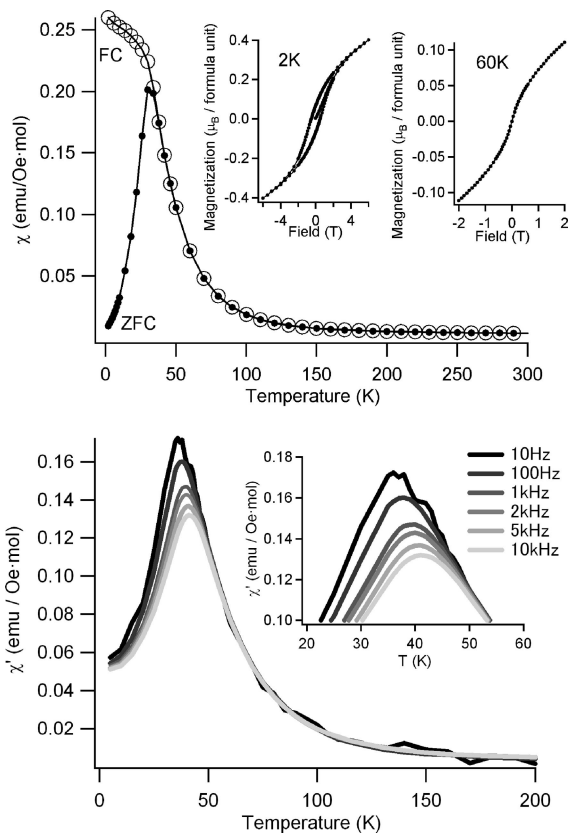


Figure 9. (a) DC magnetization data on NiCoAlO_4 platelets and (b) AC magnetic susceptibility data on the same sample.

originally derived for isolated, noninteracting particles, we turn to Stoner–Wohlfarth theory,^{33,34} where the blocking temperature of a superparamagnet is related to the particle size and intrinsic anisotropy constant by the following expression

$$E_A = KV\sin^2\theta \quad (1)$$

where K is the anisotropy constant, V is the volume of the superparamagnetic domain, and θ is the angle between the magnetization axis and easy axis of magnetization. The blocking temperature T_B is such that the product $k_B T_B$ (k_B = Boltzmann constant) is equal to the right-hand side of the expression when $\theta = 0$. Assuming that the NiCo_2O_4 platelet has a lateral area of $1\ \mu\text{m}^2$ and thickness of 50 nm, a T_B of 250 K implies an anisotropy constant K of only $0.7\ \text{erg}/\text{cm}^3$, which is perhaps 2–5 orders of magnitude smaller than what might be expected for a cobalt-containing spinel^{14,35,36} such as NiCo_2O_4 . On the other hand, if the superparamagnetic domain size is a cube that is only 50 nm tall (as thick as the platelet), then the anisotropy constant would be $270\ \text{erg}/\text{cm}^3$, which is a more reasonable value. Similarly, for the NiCoAlO_4 platelets, the low blocking temperature (40 K) implies that the superparamagnetic domain is even smaller, having a volume of 200–1000 nm³ (anisotropy values of 700–45000 erg/cm^3). Thus, within the framework of Ston-

(31) Mørup, S.; Bødker, F.; Hendriksen, P. V.; Linderroth, S. *Phys. Rev. B: Condens. Matter* **1995**, *52*, 287–294.

(32) Prené, P.; Tronc, E.; Jolivet, J.-P.; Livage, J. *IEEE Trans. Magn.* **1993**, *29*, 2658–2660.

(33) Stoner, E. C.; Wohlfarth, E. P. *IEEE Trans. Magn.* **1991**, *27*, 3475–3518.

(34) Stoner, E. C.; Wohlfarth, E. P. *Trans. R. Soc.* **1948**, *A240*, 599–644.

(35) Calero-DdelC, V. L.; Rinaldi, C. J. *Magn. Magn. Mater.* **2007**, *314*, 60–67.

(36) Zhang, H. Y.; Gu, B. X.; Zhai, H. R.; Lu, M.; Miao, Y. Z.; Zhang, S. Y.; Huang, H. B. *J. Appl. Phys.* **1994**, *75*, 7099–101.

er–Wohlfarth theory, it is more reasonable to describe each platelet as having many small superparamagnetic domains despite the apparent single-crystalline nature. The porous or rough structure of the NiCoAlO₄ platelet shown in Figure 4 shows surface protrusions that are on the order of 5–10 nm, and this or the mosaic structure may be the origin of the multiple domains. An alternate explanation would be that the large anisotropy supplies an additional easy axis of magnetization contained within the (111) plane. This causes the $\sin^2\theta$ term in 1 to become smaller than 1, because the angle between the magnetization axis and easy axis is now always less than 90°; this results in a lower blocking temperature. Hou et al. prepared single-crystal Co₃O₄ platelets approximately 20 nm thick and 200 nm in diameter, and reported a blocking temperature of approximately 35 K; however, they did not comment on whether this would be expected for the given dimensions and anisotropy constant.³⁷

Conclusions

Studying the transformation of well-defined single-crystalline layered precursors to spinels enables us to examine in detail the topochemical nature of the transformation. The spinel platelets are highly crystalline in their lateral directions, and the layered precursor method has been demonstrated to be a valuable route in preparing large, highly anisotropic superparamagnetic particles of variable composition including the metastable NiCoAlO₄. Assuming that the Stoner–Wohlfarth equation still holds for highly anisotropic particles, the surprisingly low blocking temperature of the micrometer-sized NiCoAlO₄ platelets can be explained by the presence of multiple domains induced by roughness and a mosaic structure; otherwise, the considerable shape anisotropy of the particles may be a factor.

Experimental Section

Synthesis. *Heterometal LDHs Co₂Al-LDH, NiCoAl-LDH, Ni₂Al-LDH, ZnCoAl-LDH, FeCoAl-LDH.* The precursor LDHs were prepared following the method of Liu.¹³ For heterometal LDH synthesis, nitrate salts of nickel, cobalt, and aluminum were used as precursors. The starting salts were in a M⁺²:M⁺²:Al³⁺ = 1:1:1 ratio (2.5 mmol each), and were dissolved in 500 mL of deoxygenated water. To this was added 17.5 mmol of urea, and the solution was refluxed for 48 h under nitrogen. Ni₂Al-LDH and NiCoAl-LDH were prepared on a smaller scale by dissolving the same ratio of precursors in 100 mL of water and then heating for 2 days at 190 °C (150 °C for NiCoAl-LDH) in a 120 mL Teflon-lined Parr bomb purged with nitrogen before sealing. In preparing NiCoAl-LDH, it was necessary to extensively deoxygenate the nitrate salt solution prior to the reaction, otherwise a gray powder with spinel contamination would result instead of the off-pink pure compound. After reaction, the LDH samples were washed at least twice with deionized water, at least twice with ethanol, and then dried at 60 °C in air. Conversion to spinel was conducted by heating the various LDHs at 10 °C/min to a set temperature for 12 h, and then cooling at a rate of 10 °C/min. Heat treatments at 500 °C or below were conducted under pure flowing O₂ instead of air. IR analysis on LDH precursors showed peaks at 1600 and 1490 cm⁻¹,

indicating the presence of carbonate and nitrate anions as interlayer species. Elemental analysis from ICP-AES on Co₂Al-LDH and NiCoAl-LDH yielded metal ratios of Co:Al = 1.85:1.14 and Ni:Co:Al = 1.04:1.04:1, respectively. EDS of numerous NiCoAl-LDH platelets showed a consistent elemental composition close to that obtained by ICP-AES.

Preparation of Amorphous NiCoAl-LDH. The same molar amounts of nitrate salts were dissolved in 500 mL of deoxygenated water; to this, 2.36 mL of concentrated ammonium hydroxide (14.8M, 3.5 mmol) was quickly added under a nitrogen blanket. A purple-pink suspension quickly formed, which was aged for two hours. Another 2.36 mL of ammonium hydroxide was added again, resulting in no visible change. The suspension was stirred for a final 2 h before being washed with deionized water and ethanol, during which the gel material increasingly turned darker in color to violet. Drying at 60 °C in air overnight yielded dark violet pellets, which produced a lavender powder upon grinding.

Attempted Preparation of NiCoAlO₄ from Nitrate Salts. The same amount (2.5 mmol each) of Ni(NO₃)₂·6H₂O, Co(NO₃)₂·6H₂O, and Al(NO₃)₃·9H₂O was dissolved in 10 mL of ethanol, then concentrated using a rotavap. The resulting gel was heated to 120 °C for 10 min to yield a dry magenta foam, which was calcined at 350 °C in air for 1 h, then under flowing oxygen for 12 h at 500 °C.

Attempted Preparation of NiCoAlO₄ by the Citrate Gel Method. 1.4540 g of Ni(NO₃)₂·6H₂O (5 mmol), 1.4558 g of Co(NO₃)₂·6H₂O (5 mmol), 1.8757 g of Al(NO₃)₃·9H₂O (5 mmol), 5.774 g of citric acid (6 mmol), and 2.06 mL of ethylene glycol (6 mmol) were dissolved in 10 mL of water and boiled on a hot plate. The mixture was stirred with a glass rod as a thick gel was obtained, which finally became a thick paste; this was then cooled to room temperature and ground to form a dry powder. The powder was heated in air to 450 at 20 °C/min and kept at this temperature for 6 h, during which the furnace was briefly opened once for air exchange.

α-Co(OH)₂, β-Co(OH)₂, Ni_{1/3}Co_{2/3}(OH)₂. The procedure of Liu et al. was followed,¹¹ where 2.974 g of CoCl₂·6H₂O (12.25 mmol) and 4.206 g of hexamethylenetetramine (30 mmol) were dissolved in 500 mL of a water–ethanol mixture (450 mL, 50 mL). The solution was refluxed for 1 h under nitrogen, after which the green precipitate was collected and washed with deionized water and ethanol. The product was dried at 60 °C overnight in air.

For β-Co(OH)₂, 0.8919 g of CoCl₂·6H₂O (3.75 mmol) and 0.6130 g (4.38 mmol) of hexamethylenetetraamine was dissolved in 500 mL of water, and then refluxed for 4 h to produce the pink product.

The IR spectrum of the α-Co(OH)₂ sample showed a peak at approximately 1600 cm⁻¹ (CO₃²⁻) and a broad peak centered at 3500 cm⁻¹ (hydrogen-bonded OH groups). TGA analysis also showed an extra weight loss of 10 wt%, which would be attributed to the loss of water and other interlayer species. The β form gives only a sharp peak at 3650 cm⁻¹, resulting from isolated OH groups of the Co(OH)₂ framework.

Ni_{1/3}Co_{2/3}(OH)₂ was prepared in a similar way, by dissolving 0.5948 g of CoCl₂·6H₂O (2.5 mmol) and 0.2971 g of NiCl₂·6H₂O (1.25 mmol), 0.6133 g of hexamethylenetetramine (4.38 mmol) in 500 mL of deoxygenated water and refluxing for 4.5 h under nitrogen. After the product had settled, it was washed with water and ethanol, and dried at 60 °C. Elemental analysis by ICP-AES determined the Ni:Co ratio to be 1.1:1.9.

Preparation of Isotropic NiCo₂O₄ Powder. The metal ratio was adjusted to Ni_{1.1}Co_{1.9}O₄ in order to match the stoichiometry to the NiCo₂O₄ platelet sample. Ni(NO₃)₂·6H₂O (0.6398 g; 2.2 mmol), and 1.1059 g of Co(NO₃)₂·6H₂O (3.8 mmol) were dissolved in approximately 10 mL of ethanol, which was then concentrated on

(37) Hou, Y.; Kondoh, H.; Shimojo, M.; Kogure, T.; Ohta, T. *J. Phys. Chem. B* **2005**, *109*, 19094–19098.

a rotary evaporator until a thick syrup resulted. This was dried at 120 °C and then heated in air at 350 °C for 2 h. Despite the short calcination, XRD showed the synthesis of a crystalline phase-pure spinel product, with TEM analysis showing a particle diameter of approximately 1–2 μm . A portion of this was further heated at 500 °C for 12 h under flowing oxygen.

Characterization. X-ray diffraction patterns were recorded using Cu K α radiation on a Philips X'pert MPD diffractometer. TEM images were obtained on a JEOL JEM-2010 LaB₆ microscope operating at 200kV. Thermal gravimetry and differential scanning calorimetry were conducted on a TA SDT 2960, using approximately 100 mL/min of O₂. Nitrogen adsorption measurements were obtained on a Micromeritics ASAP 2010. DC magnetization measurements were performed using a Superconducting Quantum Interference Device (SQUID) magnetometer with temperature range from 1.8 to 370 K and with a magnetic field up to 6 T. We also performed AC susceptibility measurements with the ACMS option of the Quantum Design PPMS cryostat at temperatures down to 2 K and with a frequency range from 10 Hz to 10 000 Hz. Specific heat measurements were carried out in a PPMS cryostat with He3

option with temperature down to 0.4 K using a standard semia-diabatic heat pulse technique.

Acknowledgment. The authors thank Henry Gong of the Materials Characterization Laboratory for elemental analysis and the National Science Foundation for support through Grant CHE-0616450. Electron microscopy was also supported in part by the Pennsylvania State University Materials Research Institute NanoFabrication Network and the National Science Foundation Cooperative Agreement 0335765, National Nanotechnology Infrastructure Network, with Cornell University.

Supporting Information Available: TEM images of decomposition products of NiCoAlO₄ treated at 800 °C, IR spectra of layered precursors, TGA/DSC during dehydration of layered precursors, XRD showing formation of NiCo₂O₄ platelets, magnetic measurements on isotropic NiCo₂O₄ particles, and a low-temperature heat capacity measurement of NiCoAlO₄ platelets (PDF). This material is available free of charge via the Internet at <http://pubs.acs.org>.

CM703443Q